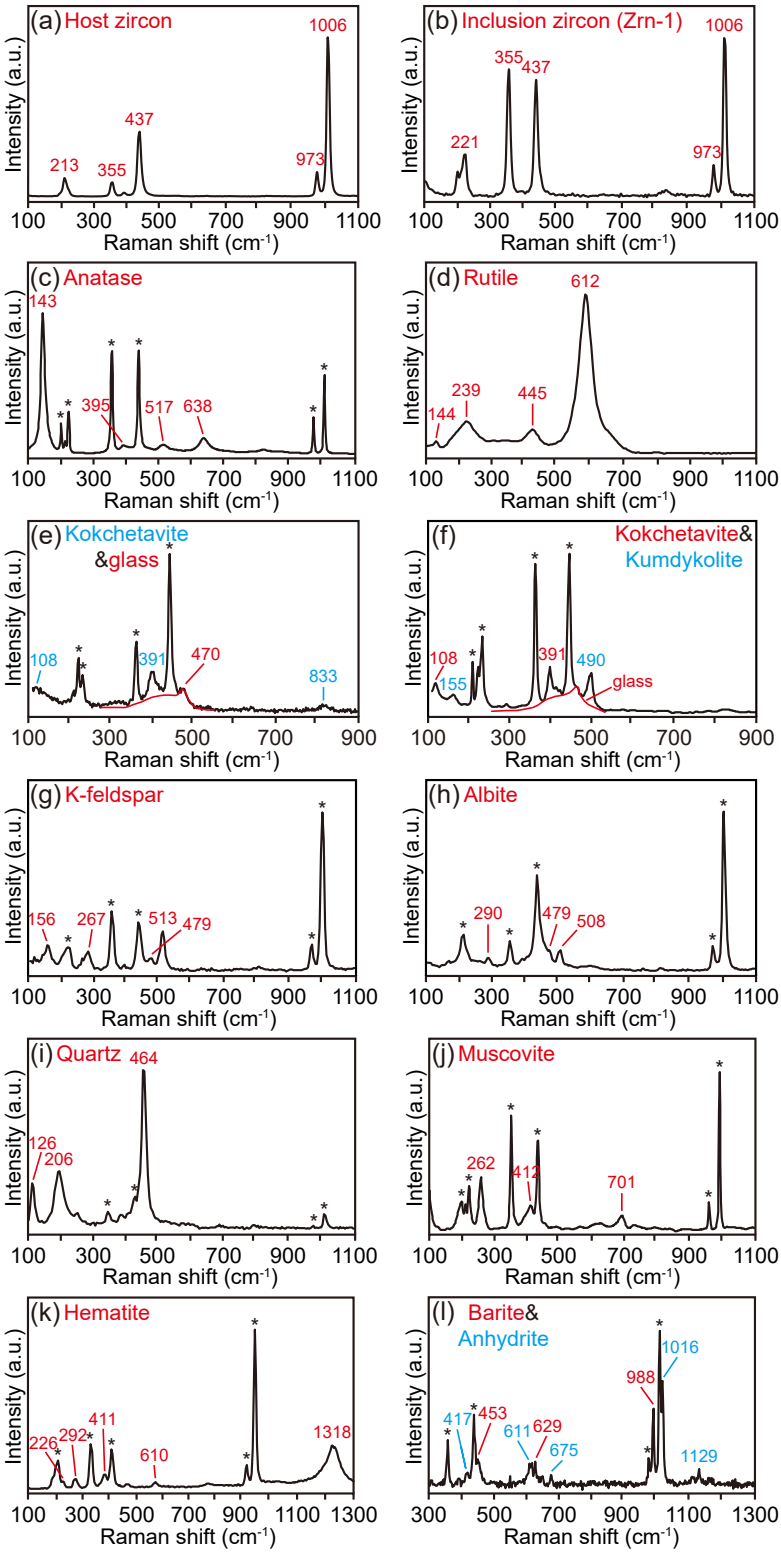

FIGURE S1. Representative Raman spectra of materials in the inclusions.

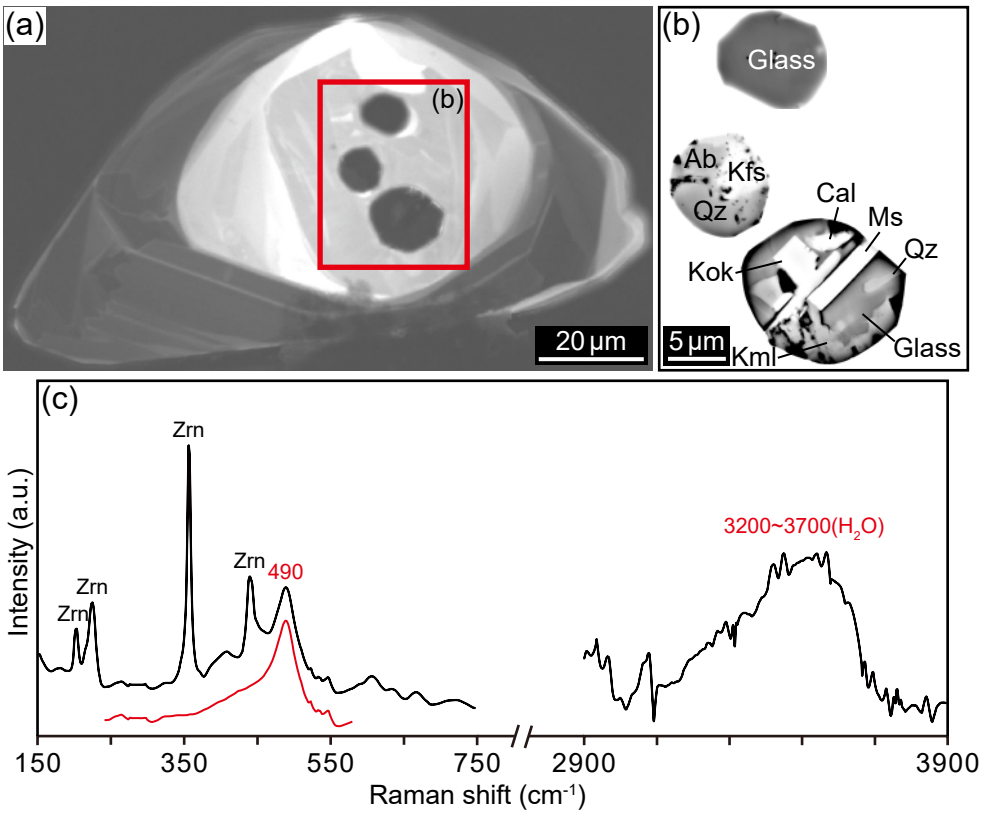

FIGURE S2. (a) CL image showing melt inclusions exposed on the polishing surface **(b)** BSE image of melt inclusions. **(c)** Raman spectra of granitic glass in melt inclusion. The glass contains H_2O with a broad band of 3200-3700 cm^{-1}, and has a granitic composition (SiO_2 = 78.23, TiO_2 = 0.07, Al_2O_3 = 12.13, FeO = 0.06, CaO = 0.21, Na_2O = 2.06, K_2O = 1.49, wt.%).

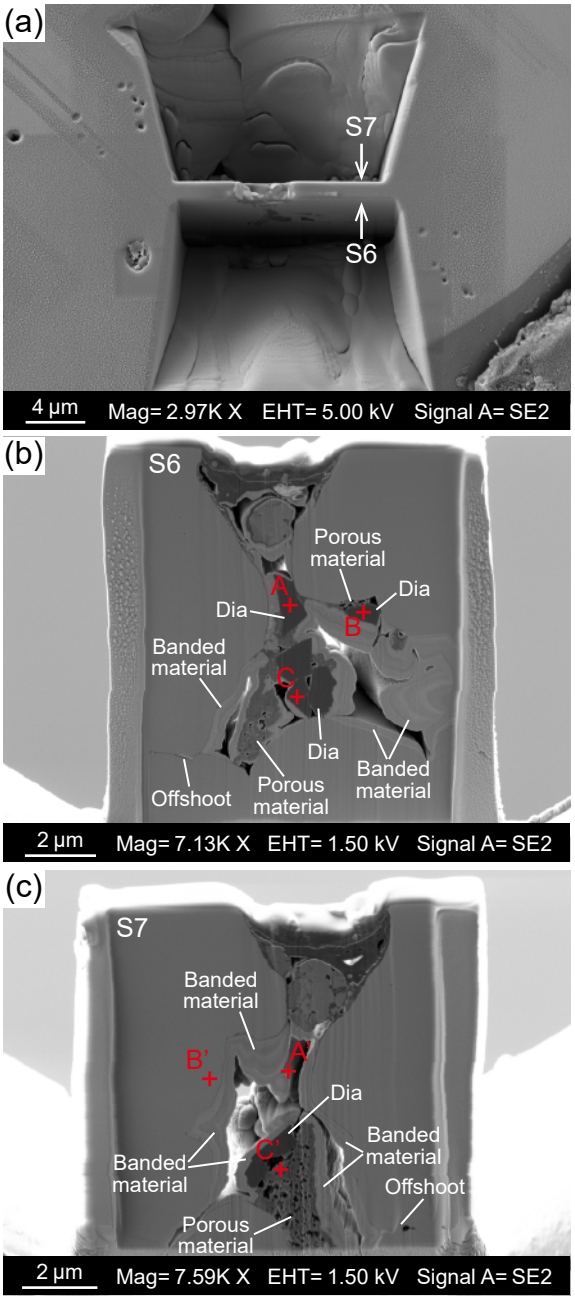

FIGURE S3. SE images obtained from inclusion 5. (**a**) SE image of air-view showing FIB-milled trench with double-sided vertical cross-sections S6 and S7. (**b** and **c**) SE images of vertical cross-sections S6 and S7. A-A', B-B' and C-C' are respectively corresponding positions on S6 and S7 cross-sections. The vertical cross-sections show that the diamonds are enclosed in the banded and porous materials.

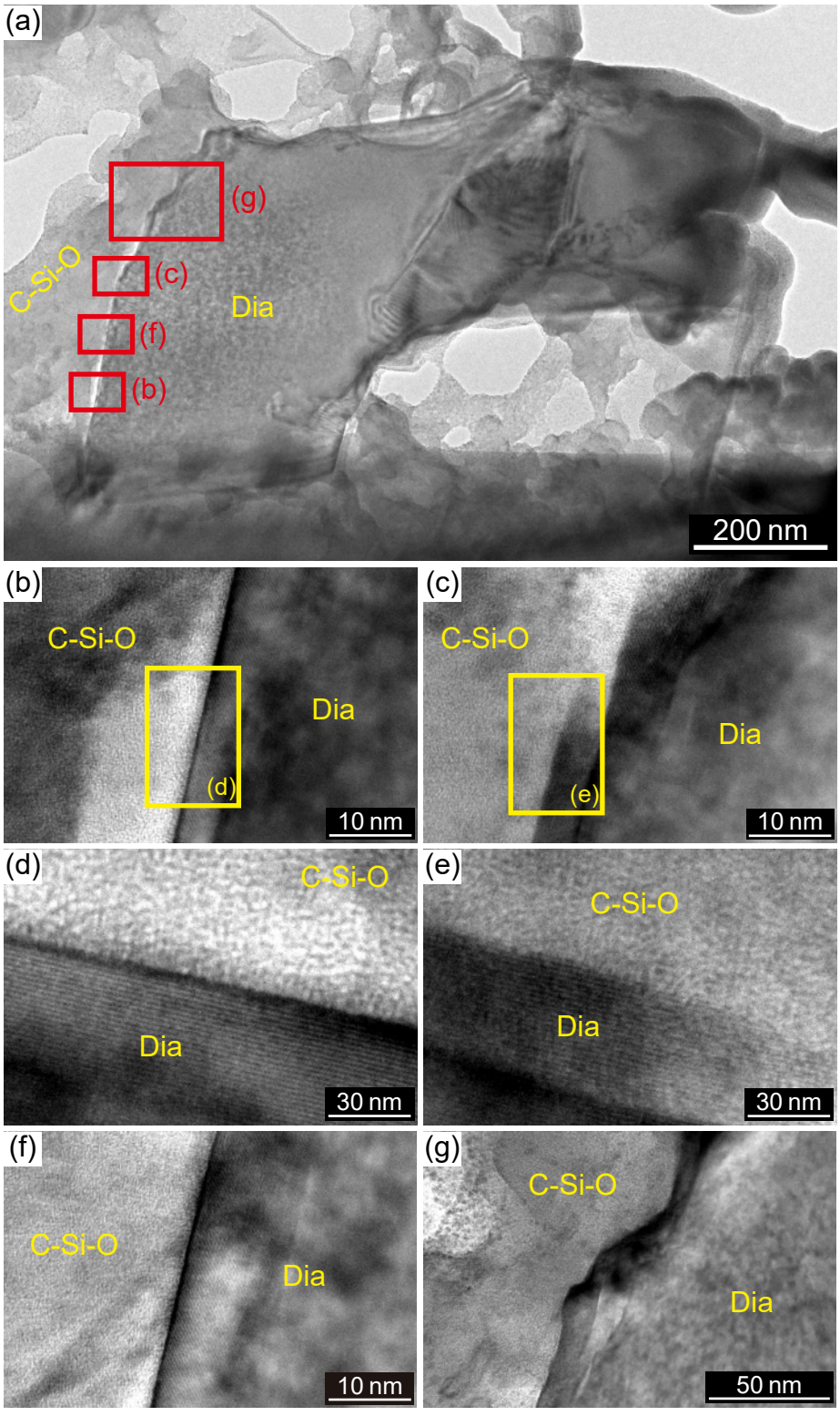

FIGURE S4. BF and HRTEM images showing fully coupled and welded interface between micrometer diamond and amorphous C-Si-O material. **(a)** BF image. **(b-g)** HRTEM images. One set of lattice fringes of diamond are present in images **b-f**. Some discrete black fringes along the interfaces arise from mass-thickness contrast.

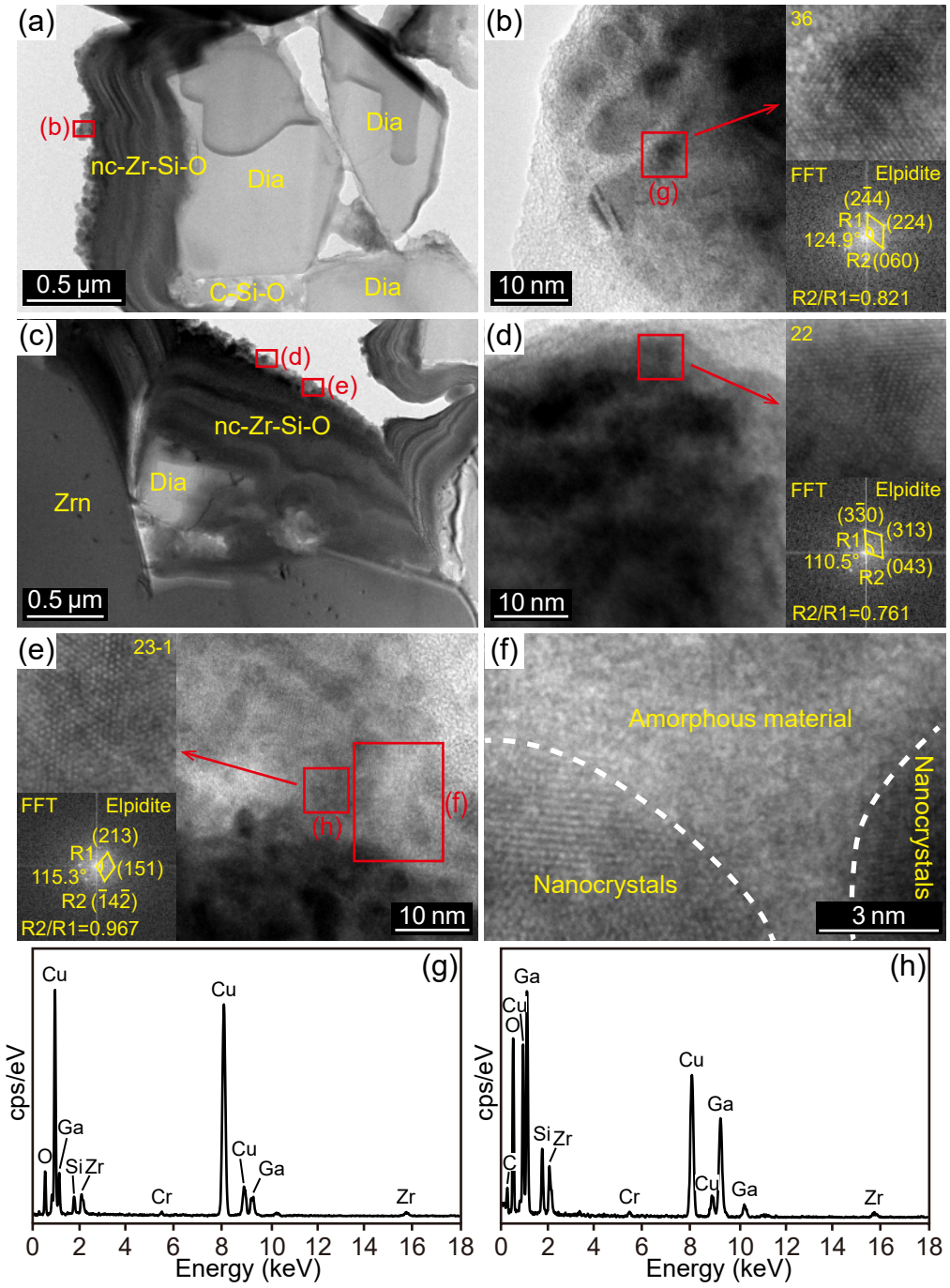

FIGURE S5. TEM observations on the nanocrystals in the banded Zr-Si-O material in inclusion 5. **(a** and **c)** BF images. **(b**, **d, e** and **f)** HRTEM images and FFT diffraction patterns. **(g** and **h)** X-ray compositional spectra of nanocrystals. The FFT diffraction patterns suggest that the nanocrystals are elpidite.

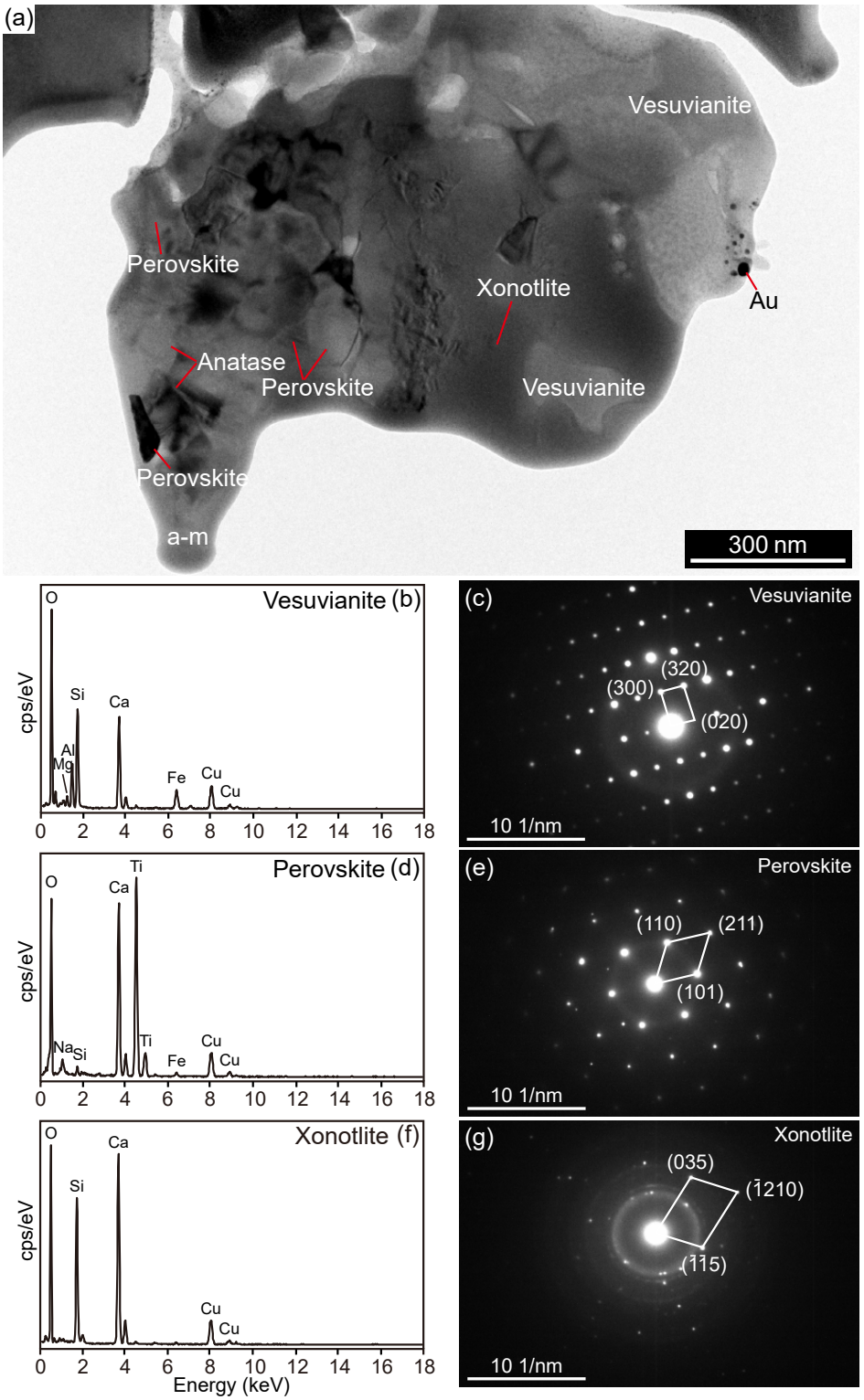

FIGURE S6. BF image, X-ray compositional spectra and SAED patterns showing the spheruite in the upper part of inclusion 5. (**a**) BF image showing nanometer minerals and amorphous material (a-m). (**b** and **c**) X-ray compositional spectrum and SAED pattern of vesuvianite. (**d** and **e**) X-ray compositional spectrum and SAED pattern of perovskite. (**f** and **g**) X-ray compositional spectrum and SAED pattern of xonolite.

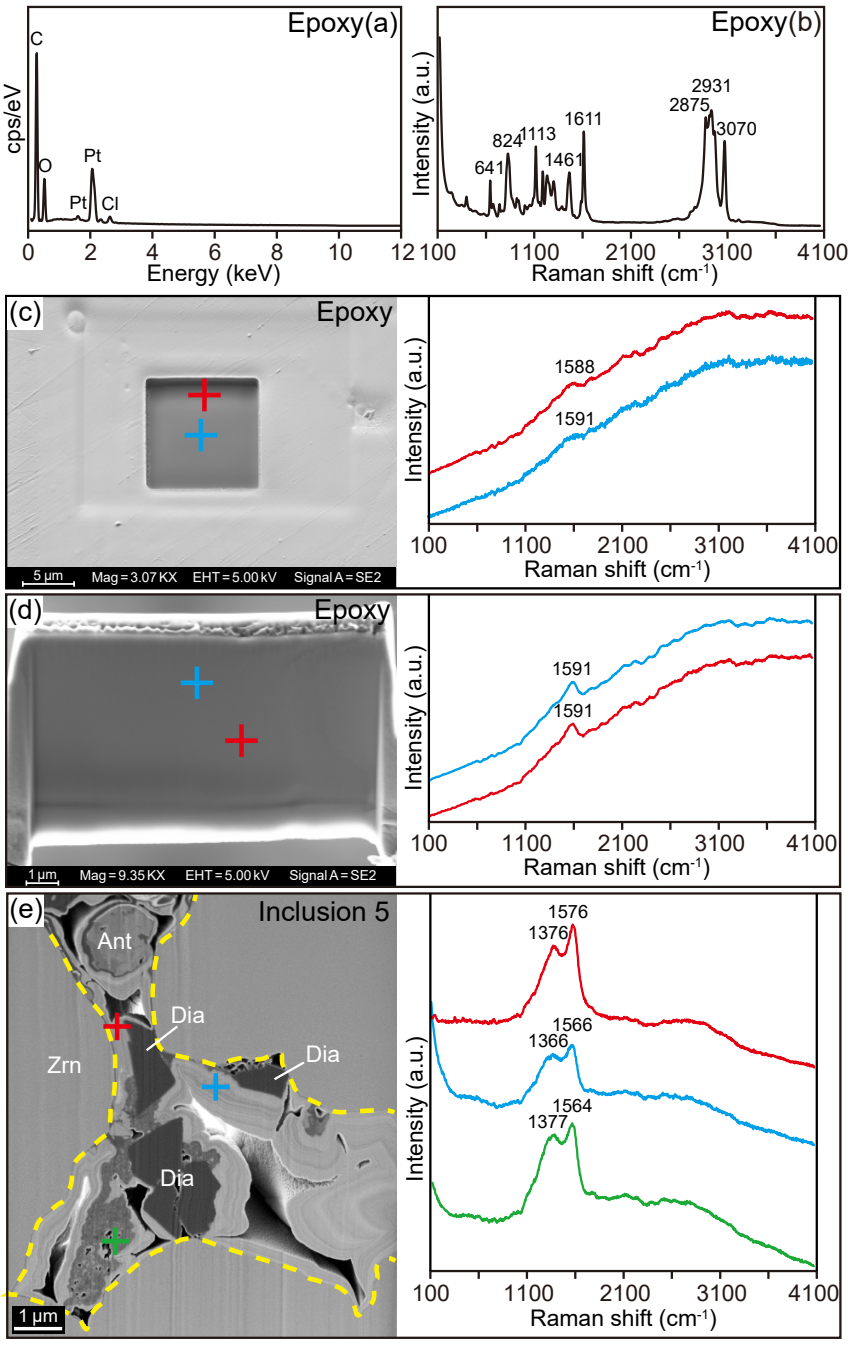

FIGURE S7. (**a**) X-ray compositional spectrum of epoxy resin, consisting of C, O and Cl. Hydrogen in epoxy resin is indicated from the Raman bands in the region of 2800-3100 cm^{-1}, which are from C-H vibrations (see plate b). Pt is from Pt coating. (**b**) Raman spectrum of the epoxy resin used in the sample preparation. (**c**) SE image showing square trench milled by FIB and Raman spectra of FIB-milling epoxy resin in the trench. The Raman signals of FIB-milling epoxy resin almost completely disappear, reflecting that the chemical bonds of epoxy resin were completely destroyed. (**d**) SE image of FIB-prepared foil of epoxy resin and Raman spectra of the foil. The thickness of the foil is about 1.5 µm. The foil only contains a weak G band, but lacks the D1 band, suggesting that there is not aromatic carbon cluster in FIB-milling epoxy resin. The SE image shows that the vertical section milled by FIB is smooth and flat, indicating that FIB milling cannot induce "evaporation" of epoxy resin. (**e**) SE image of the foil of inclusion 5 and some representative Raman spectra in the inclusion. The highly disordered CM with characteristic G and D1 bands in the sample show striking difference from FIB-milling epoxy resin.

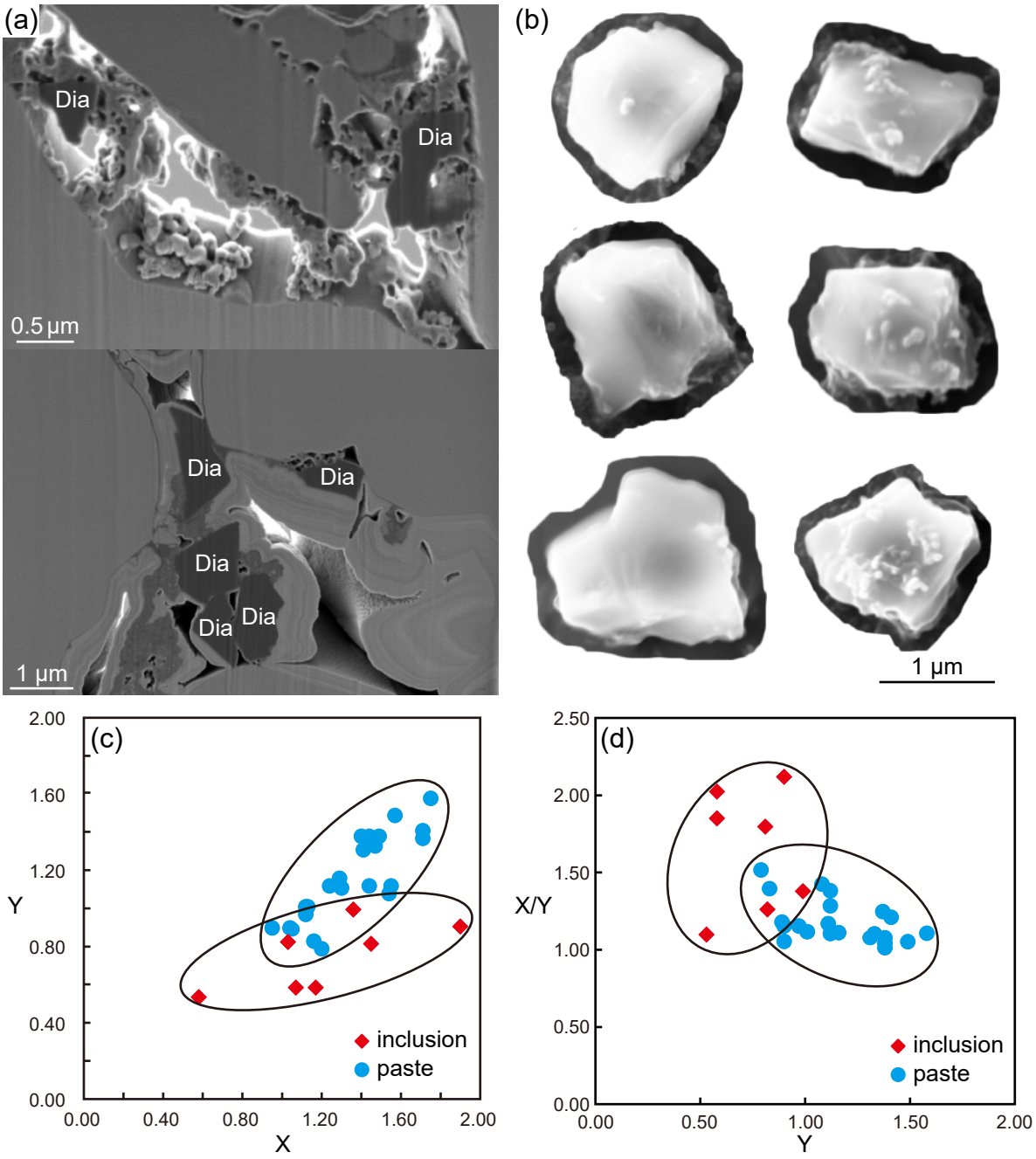

FIGURE S8. (**a**) SE images of diamonds in the inclusions. (**b**) SE images of diamonds in the paste. (**c**) and (**d**) The relationship between the major axis and the minor axis of diamond, X = the major axis, Y = the minor axis.